Journal of the American College of Cardiology
© 2014 by the American College of Cardiology Foundation
Published by Elsevier Inc.

Vol. 63, No. 19, 2014
ISSN 0735-1097/$36.00
http://dx.doi.org/10.1016/j.jacc.2014.01.055

Release and Capture of Bioactive Oxidized Phospholipids and Oxidized Cholesteryl Esters During Percutaneous Coronary and Peripheral Arterial Interventions in Humans

Amir Ravandi, MD, PhD,*† Gregor Leibundgut, MD,†‡ Ming-Yow Hung, MD,†§‖ Mitul Patel, MD,† Patrick M. Hutchins, PhD,¶ Robert C. Murphy, PhD,¶ Anand Prasad, MD,†# Ehtisham Mahmud, MD,† Yury I. Miller, MD, PhD,† Edward A. Dennis, PhD,** Joseph L. Witztum, MD,† Sotirios Tsimikas, MD†

Winnipeg, Manitoba, Canada; La Jolla, California; Basel, Switzerland; Taipei and New Taipei City, Taiwan; Aurora, Colorado; and San Antonio, Texas

Objectives This study sought to assess whether oxidized lipids are released downstream from obstructive plaques after percutaneous coronary and peripheral interventions using distal protection devices.

Background Oxidation of lipoproteins generates multiple bioactive oxidized lipids that affect atherothrombosis and endothelial function. Direct evidence of their role during therapeutic procedures, which may result in no-reflow phenomenon, myocardial infarction, and stroke, is lacking.

Methods The presence of specific oxidized lipids was assessed in embolized material captured by distal protection filter devices during uncomplicated saphenous vein graft, carotid, renal, and superficial femoral artery interventions. The presence of oxidized phospholipids (OxPL) and oxidized cholesteryl esters (OxCE) was evaluated in 24 filters using liquid chromatography, tandem mass spectrometry, enzyme-linked immunosorbent assays, and immunostaining.

Results Phosphatidylcholine-containing OxPL, including (1-palmitoyl-2-[9-oxo-nonanoyl] PC), representing a major phosphatidylcholine-OxPL molecule quantitated within plaque material, [1-palmitoyl-2-(5-oxo-valeroyl)-sn-glycero-3-phosphocholine], and 1-palmitoyl-2-glutaroyl-sn-glycero-3-phosphocholine, were identified in the extracted lipid portion from all vascular beds. Several species of OxCE, such as keto, hydroperoxide, hydroxy, and epoxy cholesteryl ester derivatives from cholesteryl linoleate and cholesteryl arachidonate, were also present. The presence of OxPL was confirmed using enzyme-linked immunoassays and immunohistochemistry of captured material.

Conclusions This study documents the direct release and capture of OxPL and OxCE during percutaneous interventions from multiple arterial beds in humans. Entrance of bioactive oxidized lipids into the microcirculation may mediate adverse clinical outcomes during therapeutic procedures. (J Am Coll Cardiol 2014;63:1961–71) © 2014 by the American College of Cardiology Foundation

From the *St. Boniface Hospital Research Centre, University of Manitoba, Winnipeg, Manitoba, Canada; †Department of Medicine, University of California-San Diego, La Jolla, California; ‡University of Basel, Basel, Switzerland; §Department of Internal Medicine, School of Medicine, College of Medicine, Taipei Medical University, Taipei, Taiwan; ‖Division of Cardiology, Department of Internal Medicine, Shuang Ho Hospital, Taipei Medical University, New Taipei City, Taiwan; ¶Department of Pharmacology, University of Colorado Denver, Aurora, Colorado; #Department of Medicine, University of Texas Health Science Center at San Antonio, San Antonio, Texas; and the **Department of Pharmacology and Chemistry and Biochemistry, University of California, La Jolla, California. This study was funded by a grant from the Swiss National Science Foundation (to Dr. Leibundgut), the Fondation Leducq, and the National Institutes of Health R01-HL119828, R01-HL093767, P01-HL055798, P01-HL088093, R01-HL086559, R01-HL081862, U54-HL119893 (to Drs. Miller, Witztum, and Tsimikas), and U54-GM069338 (Drs. Murphy, Dennis, and Witztum). Dr. Patel is on the advisory board of The Medicines Company; and is a consultant for AngioDynamics. Dr. Miller has received an investigator-initiated grant from Merck & Co., Inc. Dr. Witztum is a consultant to Isis Pharmaceuticals, Inc. and Regulus Therapeutics Inc. Drs. Witztum and Tsimikas are named as inventors on patents and patent applications for the potential commercial use of antibodies to oxidized low-density lipoprotein held by the University of California-San Diego, and receive royalties from these positions. Dr. Tsimikas is a consultant for Isis Pharmaceuticals, Inc. Genzyme, and Sanofi. All other authors have reported that they have no relationships relevant to the contents of this paper to disclose. Thomas McIntyre, PhD, has served as Guest Editor for this paper.

Manuscript received November 14, 2013; revised manuscript received January 27, 2014, accepted January 29, 2014.

JACC Vol. 63, No. 19, 2014
May 20, 2014:1961–71

Abbreviations and Acronyms

apo = apolipoprotein
CE = cholesteryl esters
HPLC = high-pressure liquid chromatography
KDdiAPC = 1-(palmitoyl)-2-(4-keto-dodec-3-ene-dioyl) phosphatidylcholine
KOdiAPC = 1-(palmitoyl)-2-(5-keto-6-octene-dioyl) phosphatidylcholine
MRM = multiple reaction monitoring
MS/MS = tandem mass spectrometry
nLDL = native low-density lipoprotein
OxCE = oxidized cholesteryl esters
OxLDL = oxidized low-density lipoprotein
OxPL = oxidized phospholipids
PAzPC = 1-palmitoyl-2-azelaoyl-sn-glycero-3-phosphocholine
PC = phosphatidylcholine
PC-OxPL = phosphocholine-containing oxidized phospholipids
PE = phosphatidylethanolamine
PGPC = 1-palmitoyl-2-glutaroyl-sn-glycero-3-phosphocholine
PONPC = 1-palmitoyl-2-(9'-oxo-nonanoyl)-sn-glycero-3-phosphocholine
POVPC = 1-palmitoyl-2-(5'-oxo-valeroyl)-sn-glycero-3-phosphocholine
PUFA = polyunsaturated fatty acid
SVG = saphenous vein graft

Cardiovascular disease remains one of the largest contributors to morbidity and mortality in the Western world (1) and is progressively increasing in developing nations. Percutaneous interventions are dominant approaches for the treatment of acute coronary syndromes and symptomatic obstructive coronary artery disease. Periprocedural complications, such as acute thrombosis and distal embolization and slow- or no-reflow phenomenon, continue to remain limitations of procedural success. For example, despite the use of optimal antiplatelet therapies and statins, a significant number of patients develop periprocedural myocardial infarction, which identifies patients at worse long-term prognosis (2). Likewise, the risk of stroke/transient ischemic attack after carotid stenting is 1% to 4%, despite the use of embolic protection devices. In renal artery interventions, worsening of blush grade or decrease in frame count, presumably caused by distal embolization, has been associated with ultrasound-detected lipid-rich plaques and suboptimal clinical response (3). Although the cause of periprocedural events is multifactorial, identification of bioactive embolized bioactive material that mediates adverse clinical events may allow the development of targeted therapies to further minimize adverse clinical events.

A large component of unstable atherosclerotic plaques is the lipid core (4), which is primarily composed of cholesterol crystals, oxidized low-density lipoprotein (OxLDL), and apoptotic and necrotic macrophage-derived foam cells (5,6). A large body of evidence shows that oxidized phospholipids (OxPL) and specifically phosphocholine-containing OxPL (PC-OxPL) play a major role in the adverse biological activities of OxLDL (7–9). PC-OxPL represent a heterogeneous group of bioactive molecules that have been shown to promote cell death, platelet aggregation (10), monocyte recruitment, and vasoconstriction. Polyunsaturated fatty acids (PUFAs) on cholesteryl esters (CE) undergo similar modifications as the PUFA on phospholipids under oxidative stress. Such oxidized cholesteryl esters (OxCE), in which the PUFA is oxidized but not the cholesterol moiety, are also abundant in OxLDL and atherosclerotic plaques (11–13) and have been shown to be biologically active, initiating proinflammatory macrophage activation and promoting foam cell formation (14,15).

Plaque components released during iatrogenic plaque rupture may result not only in mechanical obstruction because the size of the particles is larger than the microvessels but also in functional obstruction mediated by vasoconstriction, platelet aggregation, neutrophil activation, and inflammation mediated by bioactive oxidized lipids mechanically released from the site of storage or sequestration (16–18). However, oxidized lipids released during percutaneous procedures may be the most clinically relevant because they may lead to adverse clinical events. Specifically, these compounds are small enough to pass through filter devices and affect the distal vessels and microcirculation. In this study, we hypothesized that performance of percutaneous interventions results in iatrogenic plaque disruption and/or rupture leading to distal release of bioactive oxidized lipids.

Methods

See the Online Appendix.

Results

All patients underwent clinically indicated interventions. Of the 24 distal embolic protection devices analyzed, 17 FilterWire EZ (Boston Scientific, Natick, Massachusetts) systems were used in saphenous vein grafts (SVGs), 2 FilterWire EZ systems were used in the renal arteries, 2 Spider RX (ev3 Inc., Plymouth, Minnesota) systems were used in the superficial femoral arteries, and 3 Rx Accunet (Abbott Vascular, Abbott Park, Illinois) systems were used in the carotid arteries. The distal embolic protection devices were deployed before balloon angioplasty or stent placement in all cases. The first 12 filters were collected without accompanying clinical information. Table 1 represents a brief clinical background of the remaining 12 patients.

Analysis of unoxidized phospholipids and PC-OxPL. To identify PC-OxPL molecules within recovered filter material, known PC-OxPL standards PGPC, 1-palmitoyl-2-(9'-oxo-nonanoyl)-sn-glycero-3-phosphocholine (PONPC), 1-palmitoyl-2-azelaoyl-sn-glycero-3-phosphocholine (PAzPC), 1-palmitoyl-2-(5'-oxo-valeroyl)- (POVPC), 1-(palmitoyl)-2-(5-keto-6-octene-dioyl) phosphatidylcholine (KOdiAPC), and 1-(palmitoyl)-2-(4-keto-dodec-3-ene-dioyl) phosphatidylcholine (KDdiAPC) were first separated on normal-phase high-pressure liquid chromatography (HPLC) with precursor ion (m/z 184) scanning mode. Figure 1A shows the total ion chromatogram of the separated PC-OxPL standards. KOdiAPC (peak 1), PONPC (peak 2), POVPC (peak 3), KDdiAPC (peak 4), PAzPC (peak 5), and PGPC (peak 6) eluted in order of mass and polarity. Figure 1B shows the molecular ions (positive ions) derived from the elution of

Table 1 Embolic Protection Devices, Vascular Territory, and Baseline Clinical Characteristics of the Patients Undergoing Percutaneous Intervention Who Had Clinical Data Recorded

Sample	Device	Vascular Bed	Age, yrs	DM	HTN	↑LDL-Cholesterol
1	FilterWire EZ (Boston Scientific, Natick Massachusetts)	SVG	66	+	+	+
2	FilterWire EZ	SVG	65	-	+	+
3	FilterWire EZ	SVG	70	-	+	-
4	FilterWire EZ	SVG	69	+	+	+
5	FilterWire EZ	SVG	58	-	-	+
6	FilterWire EZ	Renal artery	78	+	-	+
7	FilterWire EZ	Renal artery	59	+	+	+
8	Spider RX (ev3 Inc., Plymouth, Minnesota)	SFA	71	+	+	+
9	Spider RX	SFA	80	-	-	+
10	Rx Accunet (Abbott Vascular, Abbott Park, Illinois)	Carotid	59	+	+	-
11	Rx Accunet	Carotid	68	-	+	+
12	Rx Accunet	Carotid	76	-	+	-

DM = diabetes mellitus; HTN = hypertension; SFA = superficial femoral artery; SVG = saphenous vein graft.

standards corresponding to the precursor $[M+H]^+$ that were collisionally activated to generate the phosphocholine ion at m/z 184 showing m/z corresponding to known standards. Figures 1C to 1H show the elution time for each PC-OxPL standard, with KOdiAPC having the earliest elution time with a retention time of 17.5 min and PGPC eluting last with a retention time of 23.6 min.

We next analyzed the lipid extracts from embolic filter material by precursor ion scanning (m/z 184) allowing for identification of PC-OxPL. Phosphatidylcholine (PC) eluted earliest, followed by sphingomyelin and lysoPC (Fig. 2). Extracts from filter material showed an abundance of PC-OxPL molecules compared with extracts of non-oxidized, native low-density lipoprotein (nLDL) (Fig. 2A). As an example, compounds eluting between 17.5 and 19.2 min represent a large component of fragmented PC-OxPL compared with nLDL (Fig. 2B). There were also other ions present in the plaque material not seen in nLDL (e.g., m/z 678, 822, 832, 850). Given that the other ions eluted with other PC-OxPL molecules, they likely represent both fragmented and polyoxygenated unsaturated PC molecules. For example, ion 678 on the basis of mass and the elution pattern could represent the 18:0 fatty acid in the sn-1 position with C9 aldehyde moiety in the sn-2 position.

The retention time observed for the synthetic PONPC determined by the expected [M+H]+ at m/z 650.5 (Fig. 2C) was at 18.8 min, and this specific ion transition (m/z 650→184) was present in low abundance in nLDL but the most abundant ion observed in the SVG filter material elution in this retention time region (Fig. 2B). Within plaque lipid extracts, this approach was used to identify 6 OxPL on the basis of the correlation of retention times to the oxidized standards available and to the appearance of these specific ion transitions at the appropriate retention times during analysis of the SVG material.

To increase the sensitivity by using multiple reaction monitoring (MRM) scanning, the relative mass of PC-OxPL in the filters from various vascular beds was quantified by comparing with the internal standard (1,2-dinonanoyl-sn-glycero-3-phosphocholine) that was added during lipid extraction. Figure 3 demonstrates the MRM analysis of plaque material, with peaks corresponding in retention time to known synthetic standards. OxLDL lipid extracts were analyzed in the same way. We next compared the levels of PC-OxPL within different vascular beds and OxLDL. As a percent of identified PC-OxPL, the most abundant PC-OxPL was PONPC, which represented approximately 50% of identified PC-OxPL across different vascular beds. This was also the case when lipid extracts from different vascular beds were analyzed, showing PONPC as the most abundant PC-OxPL molecule, with KDdiAPC representing the smallest fraction (Fig. 4).

By using both positive and negative ionization modes (positive for PC, sphingomyelin, and lysoPC, and negative for phosphatidylethanolamine [PE], CL, PG, PS, and PI), the total phospholipid profile in SVG samples was determined (Fig. 5A). The most abundant phospholipids were of the PC class (37.82%), followed by sphingomyelin (31.06%), PE, lysoPC, PC-OxPL, and lysoPE, with other phospholipids in lesser amounts. When compared with copper-oxidized LDL (OxLDL) (Fig. 5B), the material recovered from SVGs had increased PE levels (15.40% vs. 1.63%; $p = 0.003$). This could represent cellular debris in the recovered material because PE represents a larger portion of total phospholipids in macrophages and smooth muscle cells (19). Material from SVGs also contained more lysoPC (4.84% vs. 0.35%; $p = 0.0001$) and lysoPE (3.95% vs. 0.08%; $p = 0.0001$), but less PC-OxPL (4.61% vs. 7.65%; $p < 0.0001$) compared with OxLDL. It is important to note that the OxLDL sample had been dialyzed during preparation, leading to loss of lysoPC and possibly other phospholipid species, which influences these comparisons (20).

Additional OxPL molecular species were present in these SVG samples when detailed analysis of the liquid chromatography tandem mass spectrometry (MS/MS) data was carried out. However, on the basis of the relative abundance of an internal standard of all observed precursor ions of m/z 184, the majority of the ion current was accounted

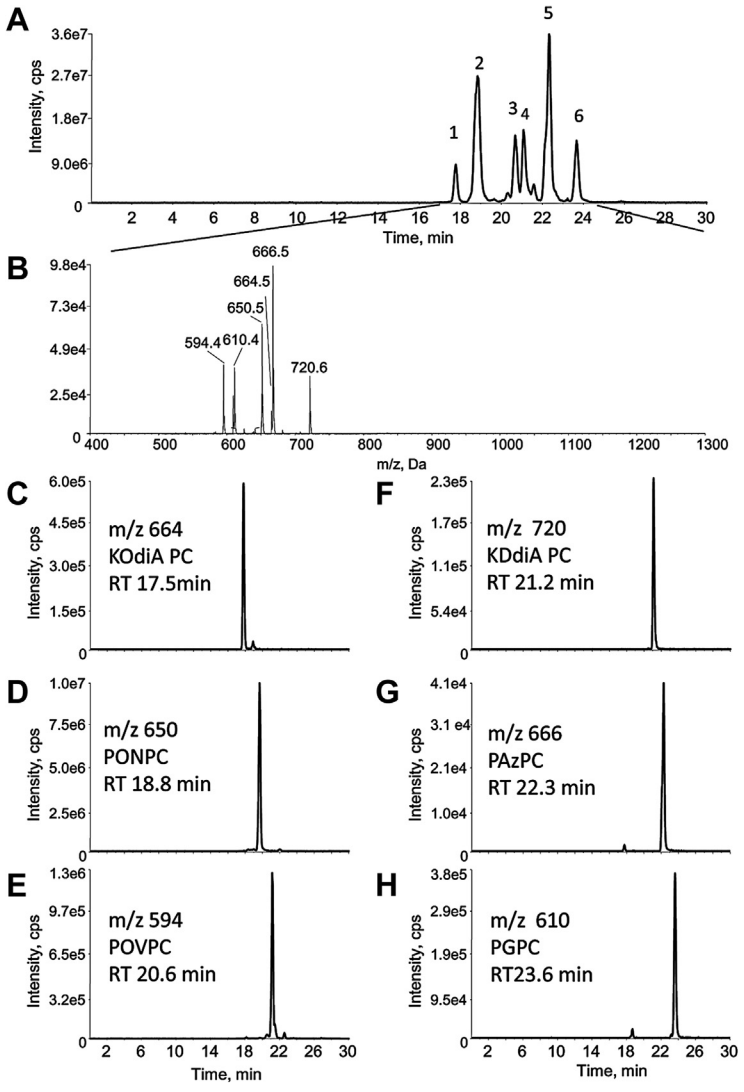

Figure 1 **Normal-Phase LC-MS/MS Analysis Standard Fragmented PC-OxPL Molecules**

(A) Total ion chromatogram from normal-phase precursor ion scan (m/z 184) liquid chromatography tandem mass spectrometry (LC-MS/MS) of 1 ng of each compound. 1-(palmitoyl)-2-(5-keto-6-octene-dioyl) phosphatidylcholine (KOdiAPC) (peak 1), 1-palmitoyl-2-(9'-oxo-nonanoyl)-sn-glycero-3-phosphocholine (PONPC) (peak 2), 1-palmitoyl-2-(5'-oxo-valeroyl)-sn-glycero-3-phosphocholine (POVPC) (peak 3), KDiAPC (peak 4), 1-palmitoyl-2-azelaoyl-sn-glycero-3-phosphocholine (PAzPC) (peak 5), and 1-palmitoyl-2-glutaroyl-sn-glycero-3-phosphocholine (PGPC) (peak 6). **(B)** Averaged mass spectra of standard fragmented phosphocholine-containing oxidized phospholipids (PC-OxPL) molecules. **(C–H)** Ion chromatographs of the synthetic standards and their specific retention times. Calibration curves on the basis of co-injection with 1,2-dinonanoyl-sn-glycero-3-phosphocholine were performed for each compound.

for by the 6 PC-OxPL described earlier. Detailed experiments are necessary to fully structurally characterize these additional species.

Analysis of OxCE. The presence of OxCE was further analyzed in 4 additional specimens using a semiquantitative HPLC-MS/MS method. Data were collected in MRM mode using transitions corresponding to CE(18:2), CE(20:4), CE(22:6), and their major oxidation products, for example, oxo-, hydroxy-, hydroxy-epoxy-, and hydroperoxy-CEs, as previously described (12,21). The chromatograms of major CE and OxCE species revealed readily detectable quantities of CE oxidation products in each of the 4 samples (Fig. 6A). The lack of positional specificity, specifically the equal abundance of 9- versus 13-hydroperoxy-linoleic CE (the 2 major peaks of the "hydroxy" series), suggested that the observed oxidation products were formed chiefly through nonenzymatic mechanisms, a result consistent with previous analyses of OxCE extracted from advanced femoral and popliteal endarterectomy specimens (12,21). However, it should be noted that this observation does not preclude a contributing enzymatic component. The extent of CE oxidation varied markedly between samples. Certain chromatograms suggested a preponderance of oxidized species (Fig. 6A, top),

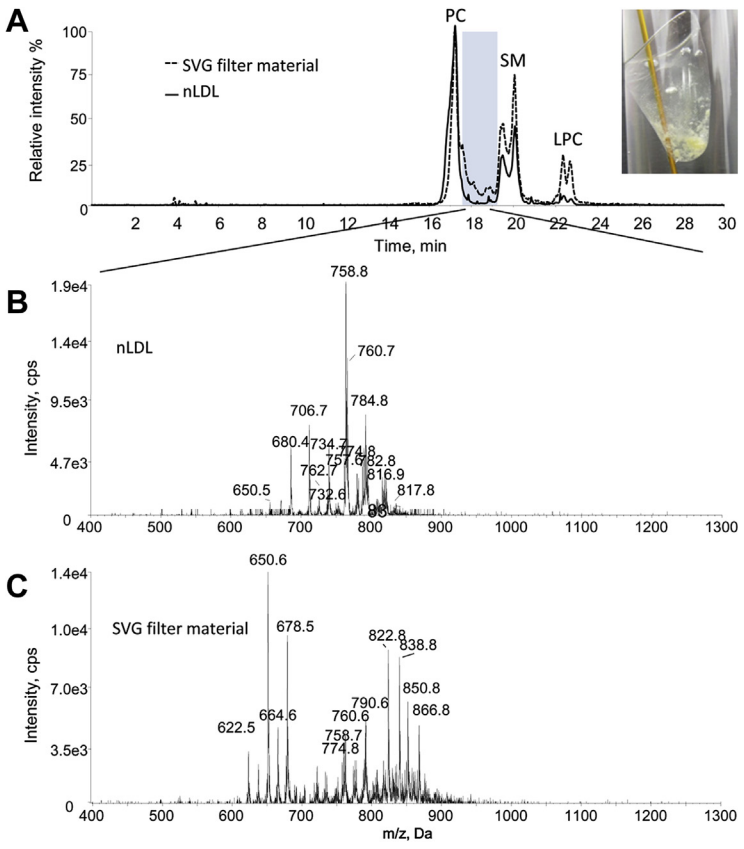

Figure 2 **Normal-Phase LC-MS/MS Analysis of Lipid Extracts From SVGs Compared With nLDL**

The filter with accompanying yellow debris is shown in the inset **(A)**. Total ion chromatogram of precursor ions (m/z 184) for plaque material **(dotted line)** and native low-density lipoprotein (nLDL) **(solid line)**. Mass spectra from retention time 17.5 to 19.2 min for nLDL **(B)** and **(C)** plaque material. lysoPC = lysophosphatidylcholine; PC = phosphatidylcholine; SM = sphingomyelin.

whereas others showed less CE oxidation (Fig. 6A, bottom). Semiquantitative analysis of these results indicated the overall content of OxCE, as a percentage of the total CE, ranged from 11% to 92% in the individual filters (Fig. 6B). Further analysis of individual CE species and their oxidation products revealed the major acyl component was 18:2 (linoleic), followed by 20:4 (arachidonic), and 22:6 (docosahexaenoic) (Fig. 6C). The relative abundance of OxCE species followed directly from this acyl distribution; oxidation products of CE(18:2) were the most abundant followed by oxidation products of the less abundant, highly unsaturated species CE(20:4) and CE(22:6).

Enzyme-linked immunosorbent assays and immunochemical staining evidence of the presence of OxPL. Complementary immunochemical techniques were used to demonstrate the presence of OxPL in the recovered plaque material, as well as the major plasma carriers of PC-OxPL, namely, lipoprotein(a) and plasminogen. This was accomplished by sonication of the filter materials in phosphate-buffered saline, which were then directly plated on microtiter well plates; the different moieties were measured by enzyme-linked immunosorbent assay techniques using antibodies specific for OxPL, apolipoprotein (apo) B-100, apo(a), and plasminogen, and the data were expressed as relative light units per 100 ms. The mean ± SD value was 11,342 ± 13,220 for OxPL, 8,114 ± 9,524 for apo(a), 6,058 ± 10,591 for apoB-100, and 2,103 ± 1,602 for plasminogen, which represent values approximately 5 times above background. Because different secondary antibodies were used in each assay, a direct comparison of the relative amounts of each component cannot be made.

Immunochemical methods also directly confirmed the presence of OxPL by immunostaining with antibody E06, which binds to the PC headgroup of oxidized but not normal phospholipids (Fig. 7). In addition, prominent staining was noted for malondialdehyde epitopes, representing another well-defined oxidation-specific epitope, in this case epitopes of unstable 3-carbon dialdehyde that binds to proteins in the lesion.

Discussion

This study documents the release and capture of OxPL and OxCE from multiple vascular beds after percutaneous

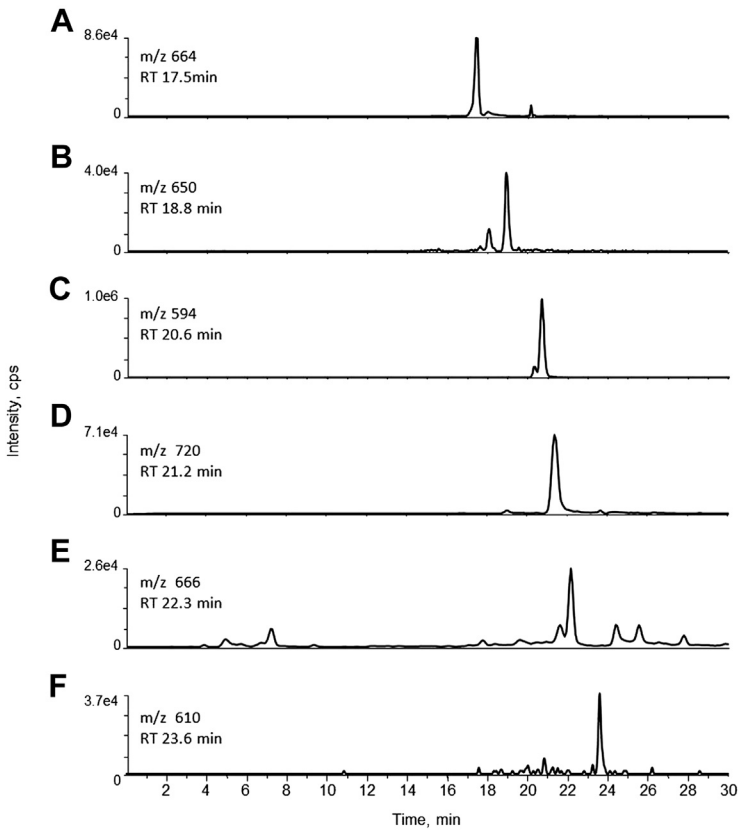

Figure 3 **Identification of PC-OxPL Molecules Within Plaque Material From Filter Retrieved From Percutaneous Coronary Intervention in Plaque Material**

Single ion chromatograms of fragmented PC-OxPL molecules within retrieved plaque material **(A)** KOdiAPC, **(B)** PONPC, **(C)** POVPC, **(D)** 1-(palmitoyl)-2-(4-keto-dodec-3-ene-dioyl) phosphatidylcholine (KDdiAPC), **(E)** PAzPC, and **(F)** PGPC. Retention times corresponded to known standards.

arterial interventions using distal protection devices in hemodynamically significant lesions from symptomatic patients. These findings were demonstrated consistently with a variety of techniques, including liquid chromatography MS/MS, enzyme-linked immunosorbent assays, and immunohistochemistry. The release of OxPL is consistent with the presence of these proinflammatory mediators in symptomatic lesions (7), the commonalities of their proatherogenic role in multiple vascular beds, and their potential role in mediating periprocedural and spontaneous clinical events.

The current study demonstrated that the majority of phospholipids identified consisted of unoxidized PC, PE, and sphingomyelin, with PC-containing OxPL representing approximately 5% of the total phospholipid content. The distribution of phospholipids present in distal protection devices was similar to in vitro–generated OxLDL, which was produced by isolating LDL from normolipidemic donors and exposing it to copper sulfate. This provides further support for evidence that OxLDL is generated in vivo and in clinically relevant lesions that drive the need for treatment (5,21). The most abundant PC-containing OxPL was PONPC, which represented approximately 50% of the entire mass of fragmented PC-containing phospholipids, and is likely derived from phospholipids containing linoleic acid on the basis of its nonanoyl component that is fragmented at the carbon double bond present at this position. Other well-characterized bioactive PC-containing OxPL also were present, including POVPC, PGPC, and KOdiAPC (7,22). Prior studies have demonstrated that these OxPL are present in OxLDL and human atherosclerotic lesions and are associated with a variety of proinflammatory and proatherogenic properties. For example, they mediate endothelial/monocyte dysfunction and bioactivity (23,24) and are important ligands for scavenger receptors on macrophages (22,25) and platelets (10), which in turn lead to foam cell formation, release of inflammatory cytokines, and platelet aggregation (5,26,27).

The current observations derived from material captured in distal protection devices are generally consistent with prior data from autopsy material or endarterectomy specimens demonstrating the presence of a variety of OxPL (26,28). The relative proportions of OxPL in different studies are

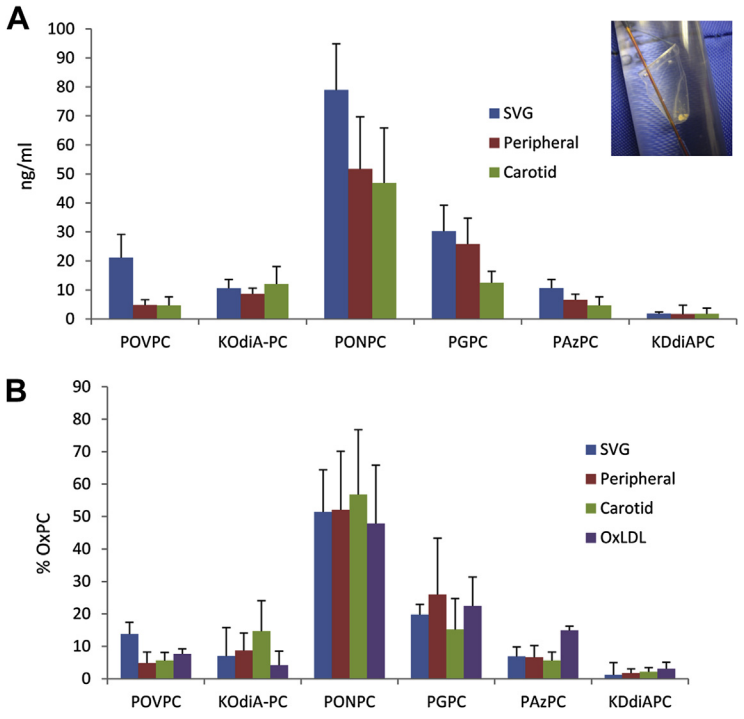

Figure 4 **Distribution of PC-OxPL Recovered From Distal Protection Filter Devices From Different Vascular Beds**

(A) Concentration of PC-OxPL within different vascular beds on the basis of dilution in 1 ml of phosphate-buffered saline before extraction. Because of larger amounts of plaque recovery from saphenous vein graft (SVG) interventions, there are higher levels of PC-OxPL within SVG samples. **(B)** Relative distribution of PC-OxPL from different vascular beds compared with OxLDL. All samples were analyzed in triplicate in normal-phase multiple reaction monitoring (MRM) LC-MS/MS (SVG: n = 5, peripheral n = 4, carotid n = 3).

somewhat different, but this may be attributed to the fact that at autopsy or during endarterectomy, the entire plaque is removed and subjected to lipid extraction, as opposed to embolic material that could represent material from the most friable part of the plaque that is released after barotrauma of the devices used to dilate the lesions. These observations also are consistent with a comprehensive immunohistological study from our group in coronary autopsy and carotid endarterectomy specimens (5), in which antibodies directed to oxidation-specific epitopes, apoB, and lipoprotein(a) were used to immunostain intimal xanthomas, pathological intimal thickening, early and late fibroatheromas, thin-cap fibroatheromas, and ruptured plaques. It was demonstrated that OxPL were present in early lesions but increased substantially in content as lesions progressed. In particular, OxPL were abundantly present in foamy macrophages, under the fibrous cap and in the necrotic core, and most prevalent in ruptured plaques. These data are consistent with our prior findings that OxPL plasma levels increase acutely after acute coronary syndromes (29) and after percutaneous coronary intervention (16) and are strongly associated with angiographically determined coronary artery disease (30) and native coronary artery chronic total occlusions (6). Furthermore, elevated levels of OxPL, as measured by the OxPL/apoB assay, independently predict 15-year cardiovascular disease event rates and reclassify approximately 30% of patients into higher- or lower-risk categories, confirming their clinical relevance (31).

The most abundant OxCE molecules present in distal protection devices were isomers of singly and doubly oxidized forms of cholesteryl linoleate CE(18:2), e.g., hydroxy- and hydroperoxy-CE(18:2). Similar oxidation products of CE(20:4) and CE(22:6) were detectable but present in lower quantities. Hutchins et al. (12) recently showed the presence of a variety of OxCE within atherosclerotic plaques from femoral artery endarterectomy specimens that represented approximately 20% of the total CE pool. They also showed that OxCEs are mainly present at the lipid core of the plaque with imaging mass spectrometry. Of note, most of the oxidized fatty acyl groups were derived from CE(18:2), but not from triglycerides in the plaques. Truncated, ω-oxidized-CEs (e.g., C9- and C5-aldehydes) and hydroxy- and hydroperoxy-CE species were identified in plaque material. In our study, aldehydes represented a minor OxCE fraction, whereas epoxy and hydroperoxy moieties constituted a majority of OxCE. This was in contrast with OxPL, the majority of which were aldehydes. This deviation in OxCE and OxPL molecular species found in distal protection devices may suggest the different mechanisms of CE and phospholipid oxidation, e.g., enzymatic versus nonenzymatic,

JACC Vol. 63, No. 19, 2014
May 20, 2014:1961–71

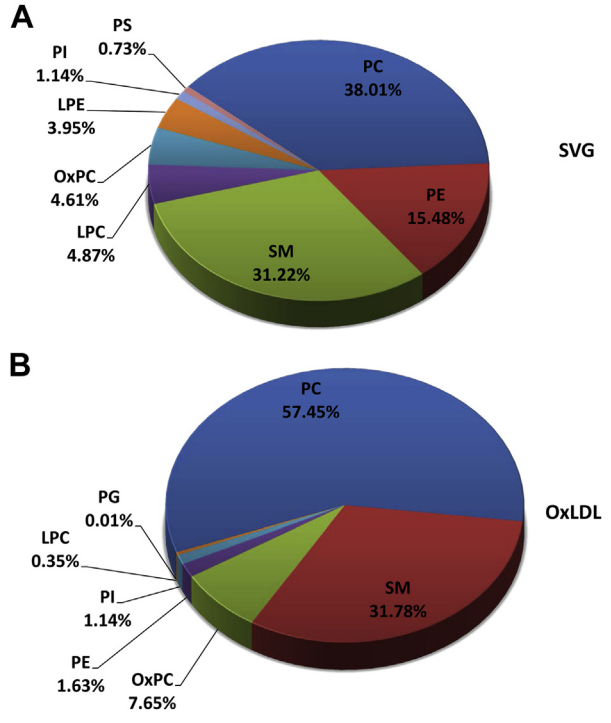

Figure 5 **Relative Total Phospholipid Composition of Embolized Material Obtained in Saphenous Vein Graft Filters And From LDL Oxidized In Vitro**

(A) Total phospholipid composition of filter material recovered from SVG interventions. The data represent an average of 4 samples analyzed in triplicate. **(B)** Samples of OxLDL also were analyzed in triplicate by normal-phase high-pressure liquid chromatography (HPLC)-MS/MS MRM scanning as a comparator. Phospholipid classes were quantitated on the basis of class-specific internal standards. Percent represents total phospholipid. LPC = lysophosphatidylcholine; PC = phosphatidylcholine; PE = phosphatidylethanolamine; PG = phosphatidylglycerol; PI = phosphatidylinositol; PS = phosphatidylserine; SM = sphingomyelin.

and/or the different susceptibility of CE and phospholipid hydroperoxides to form breakdown aldehyde products. The 18:2 and 20:4 CE are the preferential substrate for 15-lipoxygenase, the enzyme present in human atherosclerotic lesions and important in in vivo LDL oxidation, as shown in murine atherosclerosis models (32). It has also been demonstrated that once OxCE are formed, the oxidized acyl chains can be hydrolyzed from OxCE and then re-esterified into phospholipids to form OxPL (33). Further, it is also possible that enzymatic processes, mediated for example by 15-lipoxygenase, first initiate CE peroxidation and then nonenzymatic pathways predominate as the lesions progress and mature, leading to accumulation of aldehydic products. The fact that we observed no positional specificity among OxCEs suggested that nonenzymatic oxidation was dominant, but it certainly does not rule out enzymatic initiation or amplification of CE oxidation.

Clinical implications. These findings provide a novel mechanism for the benefit of distal protection devices in potentially reducing periprocedural events, by preventing embolized plaque material with its cargo of OxPL and OxCE from entering the microcirculation. OxPL have acute detrimental effects on endothelial function (7,34), including increasing permeability by breaking down cell junctions and stress fibers, releasing proinflammatory cytokines such as interleukin-8 and monocyte chemoattractant protein-1, quenching of nitric oxide, and enhancing platelet aggregation. These effects may lead to attraction of proinflammatory cells, vasoconstriction, and microvascular obstruction.

The use of distal protection devices, compared with human autopsy or endarterectomy specimens, allows plaque material to be obtained from the iatrogenic plaque rupture of specific lesions of defined geometry and potentially represents the most clinically relevant embolized debris. Furthermore, the filter pores are generally approximately 90 to 110 μm in diameter, and smaller-sized fragments and soluble mediators not attached to larger fragments will pass through the filter, as shown for oxidized lipids in venous samples collected after percutaneous coronary intervention without distal protection (5,16,29).

Clinical evidence of the potential role of CE is provided by near-infrared spectroscopy (35,36), which detects lipid-rich plaque composed mostly of CE, and by intravascular ultrasound virtual histology that detects the lipid-rich necrotic core (37). It is not known whether OxCE are imaged with near-infrared spectroscopy. This study suggests that developing techniques to image OxCE within this larger pool of cholesteryl esters may provide more precise risk stratification of periprocedural events and spontaneous plaque rupture. It would also allow performance of studies to follow the natural history of the role of oxidized lipids in clinical event prediction, similar to the PROSPECT (Predictors of Response to CRT) study (38), and to determine the efficacy of pharmacological agents. We have developed techniques to image these oxidized lipids in animal models using targeted nanoparticles containing oxidation-specific antibodies with nuclear and magnetic resonance imaging techniques (39) or using fluorescent protein-tagged oxidation-specific antibodies (40), which ultimately may be modified and coupled to invasive modalities as molecular imaging probes in humans. In animal studies of atherosclerosis regression, oxidized lipids are one of the first plaque components to disappear from the vessel wall and are subsequently replaced by collagen and smooth muscle cells as markers of plaque stabilization (40–42). Therefore, imaging changes in the oxidized lipid content of plaques may provide a unique and informative index of rapid changes in plaque composition before anatomic plaque regression, which may reflect clinical benefit.

Future studies linking release of such OxPL with periprocedural clinical events are needed to confirm this hypothesis. If this is confirmed, therapeutic agents to target oxidized lipids, such as human and "natural" oxidation-specific antibodies (9,43), could be infused during acute coronary syndrome/ST-segment elevation myocardial infarction or just before percutaneous interventions to bind the released

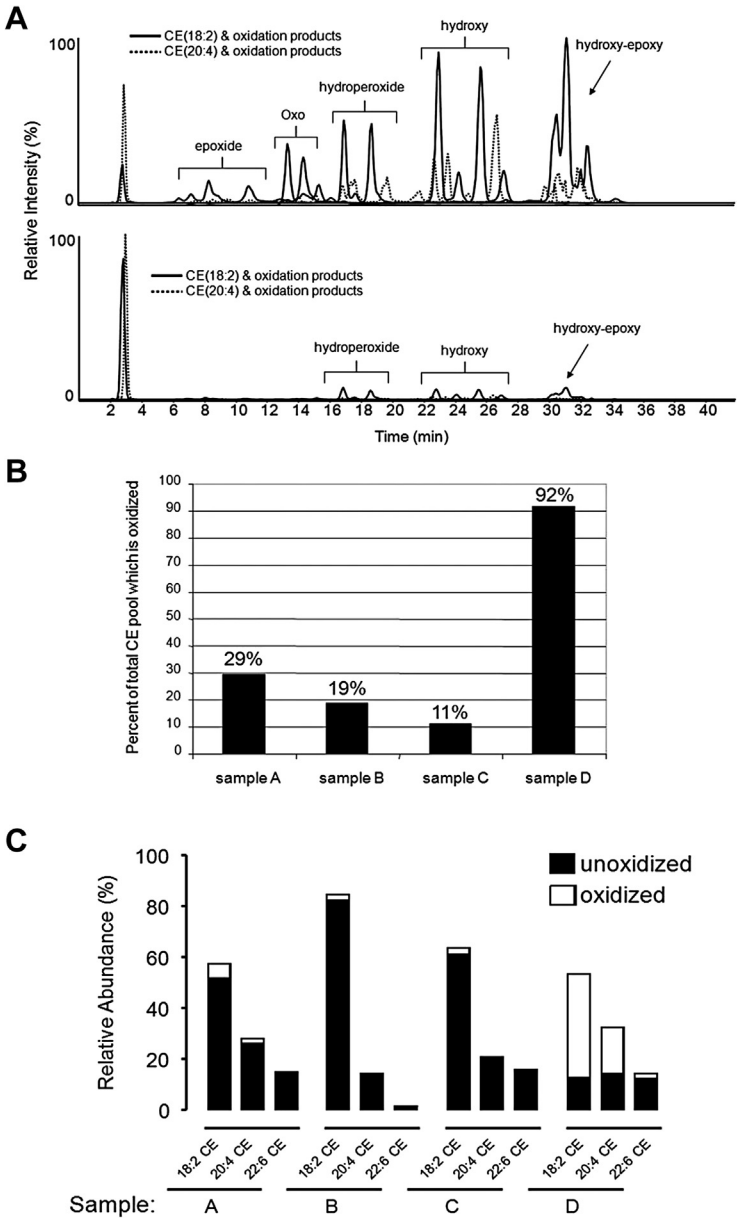

Figure 6 **Normal-Phase HPLC-MS/MS Analysis of Cholesteryl Esters Extracted From a Distal Protection Filter After Human SVG Procedure**

Data were collected in MRM mode. **(A)** Solid chromatograms show CE(18:2) and its oxidation products; dashed chromatograms represent CE(20:4) and its oxidation products. Families of structurally related oxidation products are labeled with the characteristic oxygen moiety, for example, the group of peaks labeled "hydroxy" are isomers of CE(HODE) (*solid line*) and CE(HETE) (*dashed line*). **(B)** Estimated CE oxidation as a percent of the total CE pool in SVG filter device samples is determined by peak area ratios of the 3 major cholesteryl esters (CEs) (18:2, 20:4, 22:6) and their various oxidation products by MRM analysis. **(C)** Relative quantitation was assessed by normal-phase HPLC-MS/MS as described in the Online Appendix. **Solid bars** indicate the relative abundance of the 3 major CE species; the summed oxidation products of each CE species are indicated by **open bars**.

oxidized lipids and prevent their interaction with platelets and endothelial cells, thus potentially abrogating vasoconstriction, no-reflow phenomenon, and thrombosis (16,29,30).

Study limitations. Complete oxidized lipidomics of non–PC-based OxPL was not performed, and it is possible that non–PC-based OxPL also have pathophysiological roles. However, PC-based phospholipids are in the greatest abundance and the most well characterized. Small changes in the oxidized lipid proportions may have occurred as the result of ex vivo oxidation despite the use of ethylenediaminetetraacetic acid/butylated hydroxytoluene and careful handling, as suggested by Liu et al. (44).

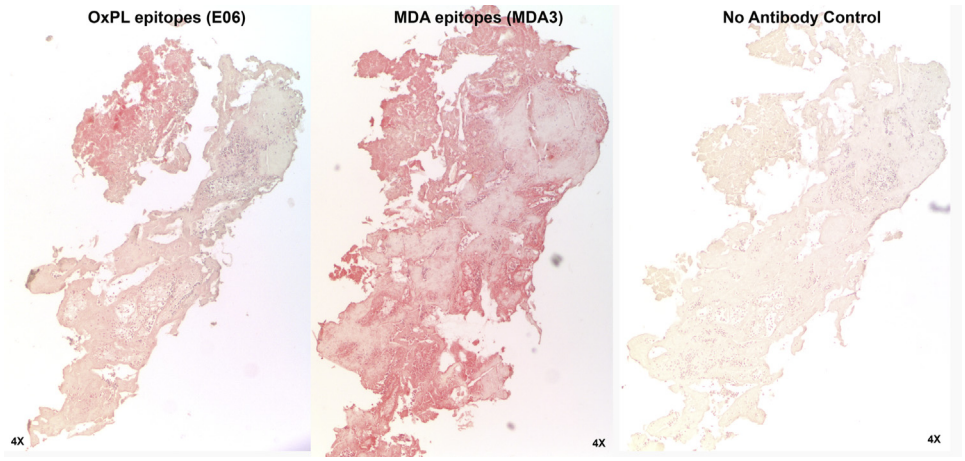

Figure 7 **Immunostaining of Material Derived From SVG Filters for OxPL Epitopes and Malondialdehyde Epitopes**

Immunostaining of material derived from SVG filters for OxPL epitopes stained with antibody E06 and malondialdehyde epitopes stained with guinea pig polyclonal antibody MDA3.

Conclusions

This study documents that OxPL and OxCE are released downstream from symptomatic lesions during percutaneous interventions from multiple arterial beds. These findings support the testable hypothesis that pre-treatment of patients undergoing such procedures with oxidation-specific antibodies to inactivate bioactive oxidized lipids released into the microcirculation may provide clinical benefit.

Reprint requests and correspondence: Dr. Sotirios Tsimikas, Vascular Medicine Program, University of California San Diego, 9500 Gilman Drive, La Jolla, California 92093-0682. E-mail: stsimikas@ucsd.edu.

REFERENCES

1. Roger VL, Go AS, Lloyd-Jones DM, et al. Heart disease and stroke statistics—2012 update. Circulation 2012;125:e2–220.
2. Wang TY, Peterson ED, Dai D, et al. Patterns of cardiac marker surveillance after elective percutaneous coronary intervention and implications for the use of periprocedural myocardial infarction as a quality metric: a report from the National Cardiovascular Data Registry (NCDR). J Am Coll Cardiol 2008;51:2068–74.
3. Prasad A, Ilapakurti M, Hu P, et al. Renal artery plaque composition is associated with changes in renal frame count following renal artery stenting. J Invasive Cardiol 2011;23:227–31.
4. Virmani R, Kolodgie FD, Burke AP, Farb A, Schwartz SM. Lessons from sudden coronary death: a comprehensive morphological classification scheme for atherosclerotic lesions. Arterioscler Thromb Vasc Biol 2000;20:1262–75.
5. van Dijk RA, Kolodgie F, Ravandi A, et al. Differential expression of oxidation-specific epitopes and apolipoprotein(a) in progressing and ruptured human coronary and carotid atherosclerotic lesions. J Lipid Res 2012;53:2773–90.
6. Fefer P, Tsimikas S, Segev A, et al. The role of oxidized phospholipids, lipoprotein (a) and biomarkers of oxidized lipoproteins in chronically occluded coronary arteries in sudden cardiac death and following successful percutaneous revascularization. Cardiovasc Revasc Med 2012;13:11–9.
7. Lee S, Birukov KG, Romanoski CE, Springstead JR, Lusis AJ, Berliner JA. Role of phospholipid oxidation products in atherosclerosis. Circ Res 2012;111:778–99.
8. Lichtman AH, Binder CJ, Tsimikas S, Witztum JL. Adaptive immunity in atherogenesis: new insights and therapeutic approaches. J Clin Invest 2013;123:27–36.
9. Miller YI, Choi SH, Wiesner P, et al. Oxidation-specific epitopes are danger-associated molecular patterns recognized by pattern recognition receptors of innate immunity. Circ Res 2011;108:235–48.
10. Podrez EA, Byzova TV, Febbraio M, et al. Platelet CD36 links hyperlipidemia, oxidant stress and a prothrombotic phenotype. Nat Med 2007;13:1086–95.
11. Fang L, Harkewicz R, Hartvigsen K, et al. Oxidized cholesteryl esters and phospholipids in zebrafish larvae fed a high cholesterol diet: macrophage binding and activation. J Biol Chem 2010;285:32343–51.
12. Hutchins PM, Moore EE, Murphy RC. Electrospray MS/MS reveals extensive and nonspecific oxidation of cholesterol esters in human peripheral vascular lesions. J Lipid Res 2011;52:2070–83.
13. Harkewicz R, Hartvigsen K, Almazan F, Dennis EA, Witztum JL, Miller YI. Cholesteryl ester hydroperoxides are biologically active components of minimally oxidized low density lipoprotein. J Biol Chem 2008;283:10241–51.
14. Choi SH, Harkewicz R, Lee JH, et al. Lipoprotein accumulation in macrophages via toll-like receptor-4-dependent fluid phase uptake. Circ Res 2009;104:1355–63.
15. Kadl A, Sharma PR, Chen W, et al. Oxidized phospholipid-induced inflammation is mediated by Toll-like receptor 2. Free Rad Biol Med 2011;51:1903–9.
16. Tsimikas S, Lau HK, Han KR, et al. Percutaneous coronary intervention results in acute increases in oxidized phospholipids and lipoprotein(a): short-term and long-term immunologic responses to oxidized low-density lipoprotein. Circulation 2004;109:3164–70.
17. Gregorini L, Marco J, Heusch G. Peri-interventional coronary vasomotion. J Mol Cell Bio 2012;52:883–9.
18. Leineweber K, Bose D, Vogelsang M, Haude M, Erbel R, Heusch G. Intense vasoconstriction in response to aspirate from stented saphenous vein aortocoronary bypass grafts. J Am Coll Cardiol 2006;47:981–6.
19. Sahu S, Lynn WS. Lipid composition of human alveolar macrophages. Inflammation 1977;2:83–91.
20. Steinbrecher UP, Parthasarathy S, Leake DS, Witztum JL, Steinberg D. Modification of low density lipoprotein by endothelial cells involves lipid peroxidation and degradation of low density lipoprotein phospholipids. Proc Natl Acad Sci U S A 1984;81:3883–7.
21. Tsimikas S, Miller YI. Oxidative modification of lipoproteins: mechanisms, role in inflammation and potential clinical applications in cardiovascular disease. Curr Pharm Des 2011;17:27–37.

22. Podrez EA, Poliakov E, Shen Z, et al. Identification of a novel family of oxidized phospholipids that serve as ligands for the macrophage scavenger receptor CD36. J Biol Chem 2002;277:38503–16.
23. Watson AD, Leitinger N, Navab M, et al. Structural identification by mass spectrometry of oxidized phospholipids in minimally oxidized low density lipoprotein that induce monocyte/endothelial interactions and evidence for their presence in vivo. J Biol Chem 1997;272:13597–607.
24. Subbanagounder G, Leitinger N, Schwenke DC, et al. Determinants of bioactivity of oxidized phospholipids: specific oxidized fatty acyl groups at the sn-2 position. Arterioscler Thromb Vasc Biol 2000;20:2248–54.
25. Boullier A, Friedman P, Harkewicz R, et al. Phosphocholine as a pattern recognition ligand for CD36. J Lipid Res 2005;46:969–76.
26. Ravandi A, Babaei S, Leung R, et al. Phospholipids and oxophospholipids in atherosclerotic plaques at different stages of plaque development. Lipids 2004;39:97–109.
27. Podrez EA, Poliakov E, Shen Z, et al. A novel family of atherogenic oxidized phospholipids promotes macrophage foam cell formation via the scavenger receptor CD36 and is enriched in atherosclerotic lesions. J Biol Chem 2002;277:38517–23.
28. Piotrowski JJ, Shah S, Alexander JJ. Mature human atherosclerotic plaque contains peroxidized phosphatidylcholine as a major lipid peroxide. Life Sci 1996;58:735–40.
29. Tsimikas S, Bergmark C, Beyer RW, et al. Temporal increases in plasma markers of oxidized low-density lipoprotein strongly reflect the presence of acute coronary syndromes. J Am Coll Cardiol 2003;41:360–70.
30. Tsimikas S, Brilakis ES, Miller ER, et al. Oxidized phospholipids, Lp(a) lipoprotein, and coronary artery disease. N Engl J Med 2005;353:46–57.
31. Tsimikas S, Willeit P, Willeit J, et al. Oxidation-specific biomarkers, prospective 15-year cardiovascular and stroke outcomes, and net reclassification of cardiovascular events. J Am Coll Cardiol 2012;60:2218–29.
32. Cyrus T, Pratico D, Zhao L, et al. Absence of 12/15-lipoxygenase expression decreases lipid peroxidation and atherogenesis in apolipoprotein e-deficient mice. Circulation 2001;103:2277–82.
33. Hutchins PM, Murphy RC. Cholesteryl ester acyl oxidation and remodeling in murine macrophages: formation of oxidized phosphatidylcholine. J Lipid Res 2012;53:1588–97.
34. Romanoski CE, Che N, Yin F, et al. Network for activation of human endothelial cells by oxidized phospholipids. Circ Res 2011;109:E27–U52.
35. Goldstein JA, Maini B, Dixon SR, et al. Detection of lipid-core plaques by intracoronary near-infrared spectroscopy identifies high risk of periprocedural myocardial infarction. Circ Cardiovasc Interv 2011;4:429–37.
36. Kini AS, Baber U, Kovacic JC, et al. Changes in plaque lipid content after short-term intensive versus standard statin therapy: the YELLOW trial (reduction in yellow plaque by aggressive lipid-lowering therapy). J Am Coll Cardiol 2013;62:21–9.
37. Claessen BE, Maehara A, Fahy M, Xu K, Stone GW, Mintz GS. Plaque composition by intravascular ultrasound and distal embolization after percutaneous coronary intervention. J Am Coll Cardiol Img 2012;5:S111–8.
38. Stone GW, Maehara A, Lansky AJ, et al. A prospective natural-history study of coronary atherosclerosis. N Engl J Med 2011;364:226–35.
39. Briley-Saebo KC, Nguyen TH, Saeboe AM, et al. In vivo detection of oxidation-specific epitopes in atherosclerotic lesions using biocompatible manganese molecular magnetic imaging probes. J Am Coll Cardiol 2012;59:616–26.
40. Fang L, Green SR, Baek JS, et al. In vivo visualization and attenuation of oxidized lipid accumulation in hypercholesterolemic zebrafish. J Clin Invest 2011;121:4861–9.
41. Torzewski M, Shaw PX, Han KR, et al. Reduced in vivo aortic uptake of radiolabeled oxidation-specific antibodies reflects changes in plaque composition consistent with plaque stabilization. Arterioscler Thromb Vasc Biol 2004;24:2307–12.
42. Tsimikas S, Aikawa M, Miller FJ Jr., et al. Increased plasma oxidized phospholipid:apolipoprotein B-100 ratio with concomitant depletion of oxidized phospholipids from atherosclerotic lesions after dietary lipid-lowering: a potential biomarker of early atherosclerosis regression. Arterioscler Thromb Vasc Biol 2007;27:175–81.
43. Tsimikas S, Miyanohara A, Hartvigsen K, et al. Human oxidation-specific antibodies reduce foam cell formation and atherosclerosis progression. J Am Coll Cardiol 2011;58:1715–27.
44. Liu W, Yin H, Akazawa YO, Yoshida Y, Niki E, Porter NA. Ex vivo oxidation in tissue and plasma assays of hydroxyoctadecadienoates: Z,E/E,E stereoisomer ratios. Chem Res Toxicol 2010;23:986–95.

Key Words: angioplasty ■ lipoproteins ■ oxidized cholesteryl esters ■ oxidized phospholipids.

APPENDIX

For an expanded Methods section, please see the online version of this article.